Clinical Biochemistry 63 (2019) 85–91

Contents lists available at ScienceDirect

Clinical Biochemistry

journal homepage: www.elsevier.com/locate/clinbiochem

MMP7 sensitivity of mutant ECM proteins: An indicator of melanoma survival rates and T-cell infiltration

Saif Zaman[a], Boris I. Chobrutskiy[a], Jay S. Patel[a], Blake M. Callahan[a], Wei Lue Tong[a], Moody M. Mihyu[a], George Blanck[a,b,*]

[a] Department of Molecular Medicine, Morsani College of Medicine, University of South Florida, Tampa, FL, United States
[b] Immunology Program, H. Lee Moffitt Cancer Center and Research Institute, Tampa, FL, United States

ARTICLE INFO

Keywords:
Extra-cellular matrix
MMP7
Mutant amino acids
Melanoma
Immune cell infiltrates

ABSTRACT

Objective: To assess the potential impact of mutant ECM amino acids (AA) on melanoma-related matrix metalloproteinase-7 (MMP7) activity.
Design and methods: We applied a novel scripted algorithm, based on the MEROPS database, to reveal mutant-dependent sensitivity changes across the cancer genome atlas, melanoma dataset.
Results: This approach revealed a strong bias in favor of mutant AA dependent protease sensitivity increases. Thus, melanoma specimens with relatively few mutations had only MMP7 mutant sensitive, ECM peptides. As mutations increased, melanoma specimens included mutant AA representing mostly increased sensitivity and a small but increasing number of mutant AA representing decreased MMP7 sensitivity. There was no detection of melanoma specimens with only decreases in MMP7 sensitivity. Furthermore, melanoma specimens with exclusively increased sensitivity and thereby only a few overall mutations represented reduced T-cell infiltrates and worse outcomes.
Conclusions: Overall, the results indicated that changes in MMP7 sensitivity, attributable to mutant AA, have the potential of identifying patients with distinct survival outcomes as well as patients with cancer specimen immune activity.

1. Introduction

Over the last decade, a vast amount of cancer mutation data has been collected and made available for numerous studies that have not been directly related to the original motivation for the tumor DNA sequencing, namely, that cataloging more potential driver mutations would enhance knowledge regarding tumor development. While this original motivation has been fruitful, the corollary studies have also led to benefits. For example, it is clear that high mutation rates are associated with a greater anti-tumor immune response [1–7], presumably, although not yet certainly due to an increased level of (effectively non-self) neoantigens stimulating the increased immune response.

One of the areas of corollary study that has been limited has been the impact of mutant amino acids on protease sensitivity [8,9]. Increased protease activity in the cancer micro-environment, and in some cases, intracellularly, is a hallmark of cancer. Extra-cellular cancer proteases are considered to be effectors of metastasis [10], and in many cases, alterations in protease activity can regulate cancer antigen presentation [11]. Thus, appreciating the impact of mutant amino acid (AA) substitutions on the activity of proteases is likely to yield benefits in understanding basic cancer development processes. Also, understanding the impact of mutant AA on protease sensitivity may provide for technical opportunities to facilitate cancer characterizations, a point of emphasis for this report. Included among the many reasons for extending the vast cancer mutant database to protease sensitivity is the ease of expanding this dimension of knowledge, owing to the fact that an extensive catalog of high quality information regarding protease binding sites has been available for decades [12,13]. In fact, effectively, protease binding quantifications in silico represented pioneering efforts in bioinformatics.

In particular, matrix metalloproteinase-7 (MMP7) has been associated with melanoma progression and invasion [14–16]. For example, Kawasaki et al. have demonstrated that MMP7 expression can be detected in 29 out 33 (87%) of melanoma samples, with 100% of

Abbreviations: BLCA, Bladder urothelial carcinoma; ECM, extra-cellular matrix; GBM, Glioblastoma multiforme; HUGO, Human genome organization; KM, Kaplan-Meier survival curve; MMP, matrix metalloproteinase; OV, Ovarian Cystadenocarcinoma; SKCM, Skin cutaneous melanoma; TCGA, The cancer genome atlas

* Corresponding author at: 12901 Bruce B. Downs Bd. MDC7, Tampa, FL 33612, United States.
E-mail address: gblanck@health.usf.edu (G. Blanck).

https://doi.org/10.1016/j.clinbiochem.2018.11.004
Received 21 August 2018; Received in revised form 30 October 2018; Accepted 6 November 2018
Available online 08 November 2018
0009-9120/

metastatic samples expressing MMP7, revealed by a retrospective Immunohistochemical study [16]. The group established MMP7 as a survival-related biomarker in melanoma, with 5-year survival rates for MMP7-positive cases being 26.3% and 5-year survival rates for MMP7-negative cases being 100% [16]. These results support the idea that MMP7 has a distinct effect on patient survival. Thus, in this report, we examined the melanoma mutant AA impacts on MMP7 sensitivity. This study is focused on the structural subset of matrisome proteins, as previously defined [17], i.e. the entire collection of proteins that are present in the ECM and have categorized the proteins into six categories: (i) glycoproteins, (ii) collagens, (iii) proteoglycans, (iv) ECM-affiliated proteins, (v) regulatory factors, and (vi) secreted proteins. In this report, we investigated the role of mutant amino acids (AA) in the ECM structural proteins. Also, melanoma was a focus because of its especially high mutation rate thereby presumably providing for many mutant matrisome coding regions, due to the randomness of mutagenesis and the large size of these coding regions [18]. Furthermore, even independently of ECM related mutagenesis, there is very little known regarding MMP7 and the ECM breakdown in melanoma, although a previous study with brain tumors clearly indicates the vulnerability of the ECM to MMP7 [19].

2. Methods

2.1. Identification and collection of mutant matrisome peptides from the TCGA and Broad databases

Naba et al. [17,20,21] have established the “matrisome”, as explained in detail in Introduction. We removed all secreted factors (i.e. hormones, interleukins) and regulatory factors (i.e. peptidases, peptidase inhibitors) from the indicated matrisome collection. We downloaded mutant AA data, for the partial matrisome, for the Broad skin cutaneous melanoma (SKCM) dataset and for the cancer genome atlas (TCGA) provisional datasets for SKCM, bladder urothelial carcinoma (BLCA), glioblastoma multiforme (GBM), and ovarian cystadenocarcinoma (OV) datasets (cBioPortal.org) [22–24]. The partial matrisome included all ECM glycoproteins, collagens, proteoglycans, and ECM-affiliated proteins, for a total of 445 ECM proteins (Table S1). Missense mutation frequencies representing either an increase or decrease in MMP7 sensitivity, according to the software described below, were counted and a “comparison of proportions” statistical test was conducted using the web tool, https://www.medcalc.org/calc/comparison_of_proportions.php.

2.2. Assessment of protease sensitivity changes due to mutant peptides

Protease cleavage matrices for MMP7 and MMP16 (matrix metallopeptidase-16) were obtained from the MEROPS Sanger Database [12] and saved in a comma-separated values file format. The protease cleavage matrices for MMP7 and MMP16 are available in the SOM (Table S2). These protease cleavage matrices were then used as an input file, along with the cBioPortal-derived, ECM mutant AA data, for the script, WholeProteanomeMutationAssesorV4.pl (Table S3). This Perl script was developed in ref. [8] to assess protease digestion potential of a peptide with a mutant AA in comparison to the same peptide with a wild-type AA sequence. The script assesses the impact of the mutant AA from one side of the MEROPs matrix to the other, i.e., over a section of eight AA. For example, the mutant is first placed at the extreme N-terminal end of the matrix, and the matrix value is calculated and compared to the calculation based on having the wild-type AA, as defined by the Uniprot database [13], in the same position. The mutant AA is then moved one position towards the C-terminal end of the matrix, and the calculations are repeated. The positions in the matrix are referred to as P4, P3, P2, P1, P1′, P2′, P3′, P4′, reflecting the direction from amino terminal to carboxy terminal, with the cut site between P1 and P1′. For each position, every AA has a numerical value. Thus, after a difference has been established for the mutant AA and the wild-type AA for each position, P4 → P4′, the value of the greatest difference is recorded. This analysis only included missense mutations. Also, mutations within eight amino acids of either terminal of the proteins assessed were not included in this analysis due to limitations of the software, WholeProteanomeMutationAssesorV4.pl. An example of the calculations of the algorithm for MMP7 is available in the SOM (Table S4).

2.3. Kaplan-Meier outcomes analyses

Clinical data, including overall and disease free survival outcomes, for the TCGA provisional SKCM dataset were downloaded from www.cBioPortal.org. Survival data were then matched to corresponding TCGA barcodes representing sensitivity differences attributed to matrisome mutations and/or the recovery of V(D)J recombination reads from exome files [25–27], as detailed in the next Methods section. Kaplan-Meier survival curves were then generated, as detailed in Results, using Graphpad Prism software.

2.4. Obtaining TRB V(D)J Recombination reads from TCGA provisional SKCM exome files

Primary and metastatic tumor, whole exome sequence (WXS) files in binary alignment map (BAM) format were downloaded from the genome data commons (GDC) to University of South Florida research computing using the GDC data transfer tool (https://gdc.cancer.gov/access-data/gdc-data-transfer-tool) with authorization via dbGaP approved project #6300 (Table S5, GDC filenames from the download manifest). Recovery of immune receptor recombination reads was performed in two stages. First, a list of candidate reads was generated using scripts described previously [25,27]. In the second step, candidate reads which contained a V region, J region, and a productive CDR3 domain were identified using novel software, available upon email request to the corresponding author. To further ensure read fidelity, the final list of productive V(D)J recombination reads was filtered to include only reads that matched both V and J regions with at least 90% nucleotide match fidelity and at least 20 nucleotide match length (Table S6).

2.5. Computational assessment of basic protease sensitivity

For a computation of basic protease sensitivity, all mutant AA are inputted into the original software, WholeProteanomeMutationAssesorV5.pl (Table S7), and a calculation is performed with the mutant AA in all positions of the matrix, respectively, to obtain a maximal score with the mutant AA, based on the MEROPS protease cleavage matrix [12,13]. That mutant AA based score is compared to the maximum score producible by the matrix. The threshold provides a selection for a percentage of the maximum score for the matrix. Example calculations are available in the SOM (Table S8).

3. Results

3.1. Melanoma mutation frequency

To determine whether there were differences in mutation frequencies, among melanoma samples, for the structural ECM proteins (Table S1), we first obtained the average number of missense mutations in the structural ECM protein coding regions for two melanoma datasets: TCGA provisional SKCM (skin cutaneous melanoma; n = 471) and Broad SKCM (n = 121) (www.cBioPortal.org) (Table S9, Table S10). There was an average of 26.2 and 24.4 missense mutations per patient barcode (sample) in the Broad SKCM and the TCGA SKCM provisional datasets, respectively. The mutation frequency for the ECM structural proteins was much lower in several other cancers: BLCA, GBM, and OV

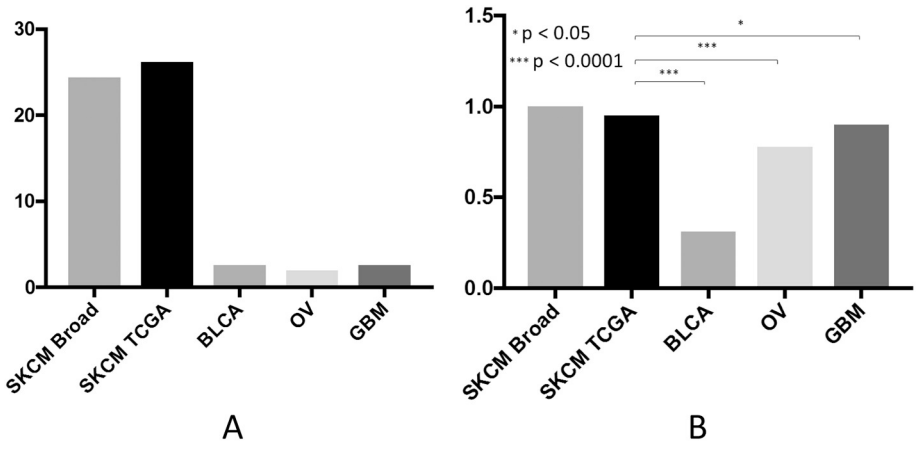

Fig. 1. High mutation frequency in ECM structural proteins in melanoma samples. (A) Average number of mutations in the extracellular matrix (ECM) structural proteins in the indicated datasets, a subset of proteins taken from a formal definition of the matrisome provided in ref. [17]. (B) Proportion of barcodes (samples) in each indicated dataset that have at least one mutation in the ECM structural proteins. A statistical comparison of the TCGA sets in the figure as follows: SKCM (skin cutaneous melanoma) when compared to BLCA ($p < .0001$), OV ($p < .0001$), and GBM ($p < .05$).

(Fig. 1A, Table S11).

One hundred percent and 95.0% of barcodes within the Broad SKCM and TCGA SKCM datasets, respectively, had at least one missense mutation in the ECM structural proteins assessed in our analysis. Consistent with our mutational frequency assessment, when comparing the proportion of barcodes with ECM missense mutations in the TCGA SKCM datasets to the TCGA BLCA ($p < .0001$), GBM ($p = .0161$), and OV ($p < .0001$) datasets, the TCGA SKCM dataset has a statistically significantly greater proportion of barcodes with ECM missense mutations in all cases (Fig. 1B, Table S11). In sum, the ECM protein coding regions are highly mutated in melanoma.

3.2. Increased MMP7 sensitivity

We next considered whether the melanoma ECM missense AA substitutions could confer increased or decreased sensitivity to MMP7, an extracellular protease associated with melanoma progression [14,15], based on an in silico protease digestion algorithm as detailed in Methods (Table S3). We first evaluated the impact of mutant AA substitutions in the ECM structural proteins in the TCGA SKCM dataset at the 0.7 threshold, i.e., the difference in the protease binding scores, represented by either the mutant AA or the wild-type AA, respectively, had to be at least 70% of the value of the AA that represents the highest score in the MMP7, MEROPs [12,13] scoring matrix (Table 1; Table S12). Results indicated a much greater number of AA substitutions that led to increased rather than decreased sensitivity ($p < .0001$). This shift towards increased MMP7 sensitivity was consistent across two thresholds, 0.7 and 0.9, the latter representing the higher standard of the requirement for a 90% increase or decrease in the score, due to the mutant AA (Table 1; Table S12). Both the TCGA and Broad SKCM (Table 1; Table S13) datasets revealed this trend towards increased sensitivity.

We next determined whether this shift towards increased protease sensitivity was specific for MMP7. We repeated the initial analysis using the MEROPS protease cleavage matrix for MMP16. Results indicated that the same set of mutant AAs that conferred a shift towards protease sensitivity for MMP7 conferred a shift towards decreased protease sensitivity for MMP16 (Table 2, Table S14).

3.3. Purely sensitive barcodes have worse outcomes

We next determined whether barcodes representing increased sensitivity towards MMP7 conferred any survival distinctions in the TCGA SKCM dataset. (No survival information was available for the Broad dataset.) We obtained survival data and matched overall survival (OS) and disease-free survival (DFS) data with the output from the protease digestion algorithm to generate KM curves. At the 0.9 threshold, of the 342 barcodes representing at least one missense AA substitution in the ECM structural proteins, 243 barcodes represented at least one missense AA substitution that increased MMP7 sensitivity. Of these 243 barcodes, most included AA substitutions representing both increased and decreased MMP7-sensitivity, respectively. Thus, we identified the barcode set that excluded all barcodes with no mutations for the ECM structural proteins (ECM; Table S1) and excluded all barcodes with (multiple) AA substitutions representing increased and decreased MMP7 sensitivity. This set of 56 barcodes, with only AA substitutions representing an increase in MMP7 sensitivity at the 0.9 threshold, also represented a worse OS and DFS when compared to all remaining TCGA SKCM barcodes (Fig. 2A, B). The mean survival periods and p-values for the log-rank tests are given in the legend for Fig. 2. The full Graphpad Prism output for Fig. 2A is available in the SOM (Table S15). These OS and DFS results were consistent for both the 0.9 and 0.7 thresholds (Fig. 2C, D).

3.4. Recovery of TRB recombination reads in WXS representing the distinct classes of MMP7, mutant ECM sensitivity changes

Previous work has established the recovery of TRB recombination reads from WXS files as an assay for the presence of T-cells in tumor specimens, for examples, refs. [27, 28]. Given the association between

Table 1
A breakdown of protease sensitivity data, representing the TCGA and Broad datasets for melanoma (SKCM), for MMP7 and the ECM structural proteins, using WholeProteanomeMutationAssesorV4.pl. As described in detail in the text, the WholeProteanomeMutationAssesorV4.pl software establishes a change in protease sensitivity, according to the MEROPS binding matrix [12,13] for that protease, in this case MMP7. Additional details available in Tables S12, S13.

	0.7 Threshold			0.9 Threshold		
Dataset	Number of mutant AA substitutions that confer decreased sensitivity	Number of mutant AA substitutions that confer increased sensitivity	p-Value	Number of mutant AA substitutions that confer decreased sensitivity	Number of mutant AA substitutions that confer increased sensitivity	p-Value
SKCM TCGA	283	1126	2.327E−05	101	1071	1.555E−07
SKCM Broad	373	1450	2.724E−07	31	298	7.961E−09

Table 2
A breakdown of protease sensitivity data, representing the TCGA dataset for melanoma (SKCM), for MMP7 and MMP16 and the ECM structural proteins, using WholeProteanomeMutationAssesorV4.pl. As described in detail in the text, the WholeProteanomeMutationAssesorV4.pl software establishes a change in protease sensitivity, according to the MEROPS binding matrix [12,13] for that protease, in this case MMP7 and MMP16. Additional details available in Tables S12, S14.

	0.7 Threshold			0.9 Threshold		
Protease	Number of mutant AA substitutions that confer decreased sensitivity	Number of mutant AA substitutions that confer increased sensitivity	p-value	Number of mutant AA substitutions that confer decreased sensitivity	Number of mutant AA substitutions that confer increased sensitivity	p-Value
MMP7	283	1126	2.327E−05	101	1071	1.555E−07
MMP16	1288	717	0.0405	712	148	1.092E−05

the ECM and lymphocyte infiltration/activation [29,30], we searched TCGA SKCM WXS files for the presence of TRB recombination reads, as described in Methods. Our initial results indicated that barcodes representing the presence of the TRB recombination reads had a significantly improved OS and trended towards a better DFS (Fig. 3A, B), not surprising for melanoma.

We next sorted TRB recombination read-positive barcodes based on whether they were recovered from the WXS files representing the group of 56 barcodes that represented only AA substitutions that conferred increased MMP7 sensitivity (Fig. 2A, Table S16). Results indicated that barcodes with only an increase in MMP7 sensitivity but without the presence of TRB recombination reads had worse survival outcomes than barcodes with TRB recombination reads present (Fig. 3C–G). The mean survival periods and p-values for the log-rank tests are given in the legend for Fig. 3. The full Graphpad output for Fig. 3C, D is available in the SOM (Table S17).

3.5. Barcodes representing only MMP7 sensitive mutant peptides and TRB read recovery also represent a higher mutation rate

Previous work has indicated that T-cell infiltrates are associated with higher mutation rates, in both humans and in a mouse model [1,7]. We thus determined the average number of mutations among the ECM structural protein coding regions (Table S1) for barcodes that represented only an increase in sensitivity to MMP7, and the presence of TRB recombination reads, for comparison to the average number of mutations for barcodes that represented only an increase in sensitivity to MMP7 and the absence of TRB recombination reads. Results indicated that barcodes representing the presence of TRB recombination reads had a statistically significantly higher mutation rate than the barcodes without TRB recombination reads (Table 3, Table S18). In short, barcodes representing fewer mutations, among the ECM structural protein coding regions, had a reduced T-cell infiltrate.

3.6. Absolute MMP7 sensitivity is not correlated with a survival distinction

To determine whether the absolute sensitivity of mutant peptides could be contributing to the distinct survival differences, we designed a protease digestion algorithm that calculated a MEROPS-based score for the mutant peptide sequences. This protease digestion algorithm calculated a score for each mutant peptide and compared that score to the maximum score possible for the MMP7, MEROPS quantification matrix (Table S2). Using the same set of TCGA SKCM barcodes and same set of ECM proteins used in the previous analyses, results indicated that 132 barcodes represented at least one AA substitution among the ECM structural proteins that represented a minimum of 70% of the maximum score possible with the MMP7 matrix (Table S19). When compared to all remaining barcodes, these 132 barcodes do not represent statistically significant survival differences (Fig. S1A, S1B).

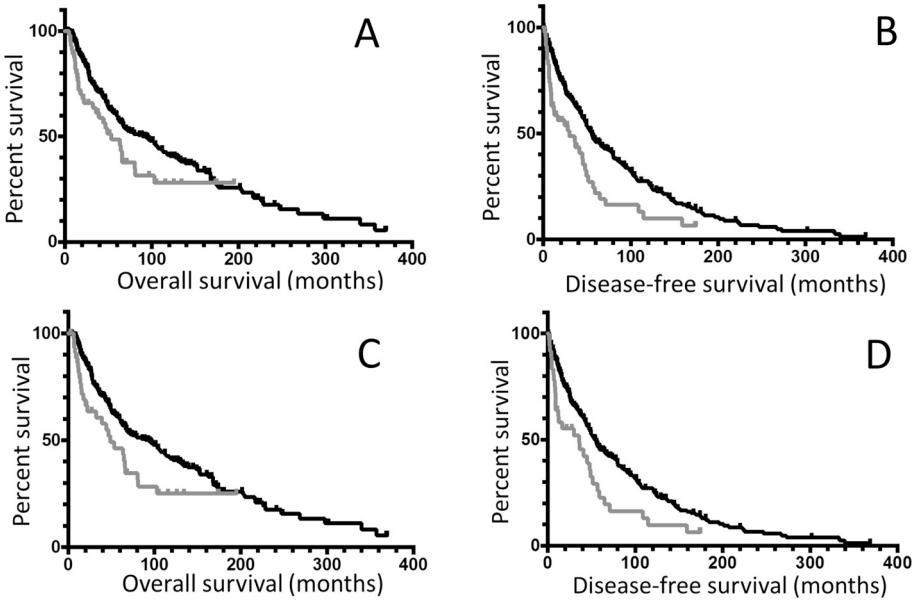

Fig. 2. Kaplan-Meier curves representing exclusively an increase in sensitivity to MMP7. (A) Kaplan-Meier (KM) overall survival (OS) curve for TCGA SKCM barcodes that represent only increased sensitivity to MMP7 at the 0.9 threshold (n = 56, gray), compared to the OS for all remaining barcodes (n = 404, black). Median OS for the barcodes representing increased sensitivity to MMP7, 53.48 months; median OS for all remaining barcodes, 92.94 months. Log rank comparison p-value, p = .027. (B) KM disease-free survival (DFS) curve for TCGA SKCM barcodes that represent exclusively increased sensitivity to MMP7 at the 0.9 threshold (n = 46, gray), compared to the DFS for all remaining barcodes (n = 354, black). Median DFS for the barcodes representing increased sensitivity to MMP7, 29.83 months; median DFS for all remaining barcodes, 55.49 months. Log rank comparison p-value, p = .0008. (C) KM OS curve for skin SKCM barcodes that represent purely increased sensitivity to MMP7 at the 0.7 threshold (n = 45, gray), compared to the OS for all remaining barcodes (n = 415, black). Median OS for the barcodes representing increased sensitivity to MMP7, 48.82 months; median OS for all remaining barcodes, 92.94 months. Log rank comparison p-value, p = .0178. (D) KM DFS curve for SKCM barcodes that represent purely increased sensitivity to MMP7 at the 0.7 threshold (n = 36, gray), compared to the DFS for all remaining barcodes (n = 364, black). Median DFS for the barcodes representing increased sensitivity to MMP7, 35.87 months; median DFS for all remaining barcodes, 54.80 months. Log rank comparison p-value, p = .0058. Note, the number of barcodes decreases, for barcodes representing exclusively sensitive AA, when the threshold is lowered, because the lower threshold then "captures" some mutant AA substitutions that, at that lower threshold, represent a decrease in MMP7 sensitivity. Those mixed sensitivity barcodes are then removed from the assessments (i.e., in Fig. 2C, D).

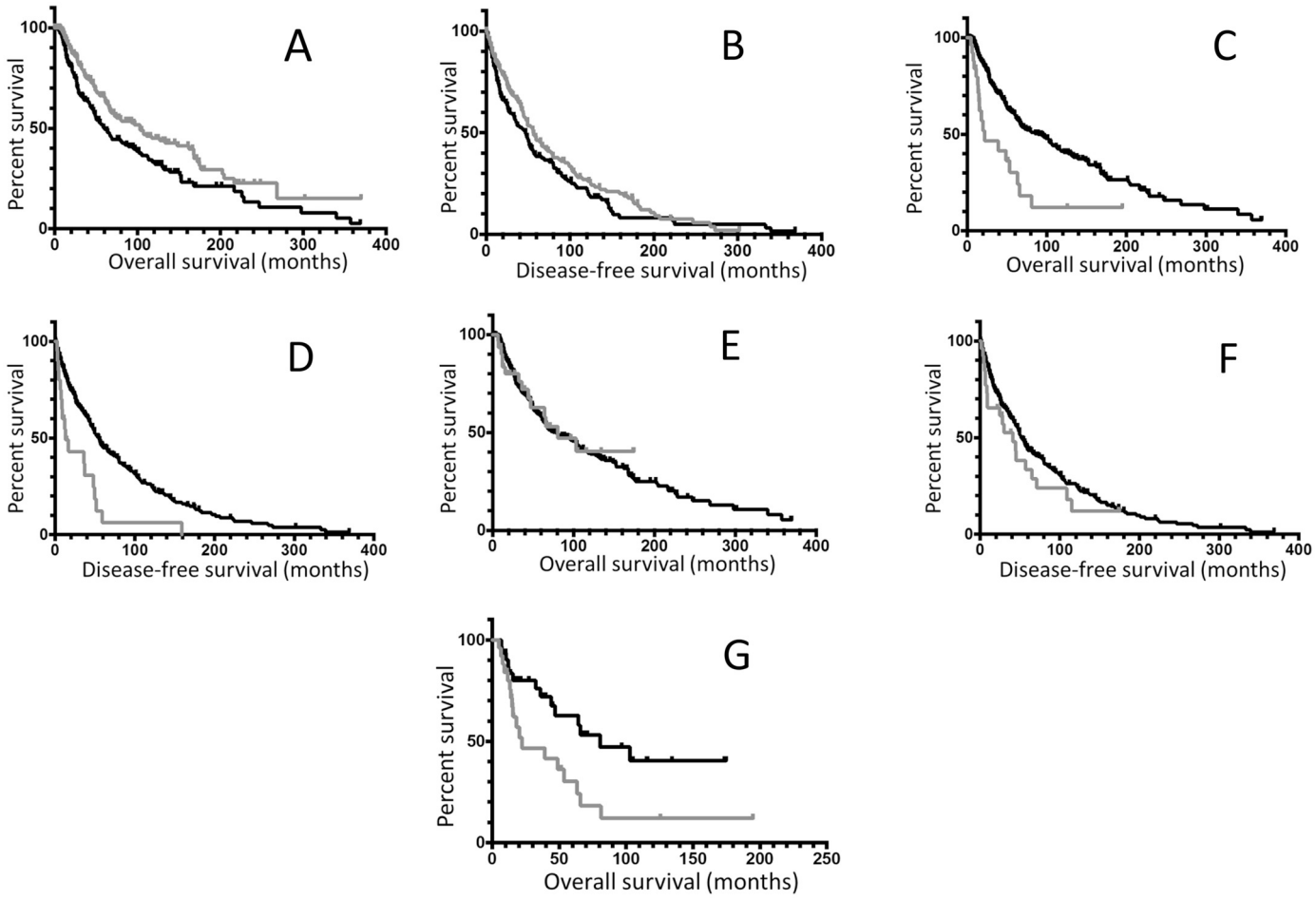

Fig. 3. Kaplan-Meier curves representing a distinct increase in sensitivity to MMP7 and VDJ recombination read count recovery. (A) KM OS curve for TCGA SKCM barcodes that were positive for TRB VDJ recombination reads (n = 247, gray), compared to the OS for all remaining barcodes (i.e., negative for TRB VDJ recombination reads; n = 213, black). Median OS for the barcodes positive for the TRB VDJ recombination reads, 103.12 months; median OS for all remaining barcodes, 60.18 months. Log rank comparison p-value, p = .0022. (B) KM DFS curve for TCGA SKCM barcodes that are positive for TRB VDJ recombination reads (n = 221, gray), compared to the DFS for all remaining barcodes (n = 179, black). Median DFS for the barcodes positive for TRB VDJ recombination reads, 56.01 months; median DFS for all remaining barcodes, 47.11 months. Log rank comparison p-value, p = .0787. (C) KM OS curve for TCGA SKCM barcodes that represented only increased sensitivity to MMP7 (at the 0.9 threshold) and are negative for TRB VDJ recombination reads (n = 25, gray), compared to the OS for all remaining barcodes (n = 435, black). Median OS for the barcodes that represent increased sensitivity to MMP7 and negative for TRB VDJ recombination reads, 22.11 months; median OS for all remaining barcodes, 89.06 months. Log rank comparison p-value, p < .0001. (D) KM DFS curve for TCGA SKCM barcodes that represented only increased sensitivity to MMP7 (at the 0.9 threshold) and negative for TRB VDJ recombination reads (n = 20, gray), compared to the DFS for all remaining barcodes (n = 380, black). Median DFS for the barcodes that represent increased sensitivity to MMP7 and negative for TRB VDJ recombination reads, 12.61 months; median DFS for all remaining barcodes, 54.80 months. Log rank comparison p-value, p < .0001. (E) KM OS curve for TCGA SKCM barcodes that represented only increased sensitivity to MMP7 (at the 0.9 threshold) and positive for TRB VDJ recombination reads (n = 31, gray), compared to the OS for all remaining barcodes (n = 429, black). Median OS for the barcodes that represented only increased sensitivity to MMP7 and are positive for VDJ recombination reads, 80.62 months; median OS for all remaining barcodes, 78.91 months. Log rank comparison p-value, p = .8558. (F) KM DFS curve for TCGA SKCM barcodes that represented only increased sensitivity to MMP7 at the 0.9 threshold and positive for TRB VDJ recombination reads (n = 26, gray), compared to the DFS for all remaining barcodes (n = 374, black). Median DFS for the barcodes that represent only increased sensitivity to MMP7 and positive for TRB VDJ recombination, 40.97 months; median DFS for all remaining barcodes, 51.48 months. Log rank comparison p-value, p = .2087. (G) KM OS curve for TCGA SKCM barcodes that represented only increased sensitivity to MMP7 (at the 0.9 threshold) and negative for TRB VDJ recombination reads (n = 25, gray), compared to the OS for SKCM barcodes that represented only increased sensitivity to MMP7 and positive for VDJ recombination reads (n = 31, black). Median OS for the barcodes that represent only increased sensitivity to MMP7 and negative for VDJ recombination reads, 22.11 months; median OS for the barcodes that represented only increased sensitivity to MMP7 and positive for VDJ recombination, 80.62 months. Log rank comparison p-value, p = .0148.

Table 3
Average number of mutations per barcode for barcodes that have at least one MMP7-sensitive mutation in the ECM structural proteins (Table S1) and are positive for TRB VDJ recombination reads vs. barcodes that have at least one MMP7-sensitive mutation in the ECM structural proteins but are negative for TRB VDJ recombination reads. Details regarding the recovery of TRB VDJ recombination reads are available in Tables S6, S16, and S18.

MMP7-sensitive with TRB	MMP7-sensitive without TRB	p-Value
14.19	8.92	0.0013681

4. Discussion

The above bioinformatics analyses indicated that mutant AA in the ECM structural proteins lead, far more often than not, to an increase in MMP-7 sensitivity. However, an increase in sensitivity, particularly with the algorithm used to detect this increase, does not necessarily indicate that the mutant AA has the effect of making peptides with those mutant AA highly sensitive to MMP7. In fact, when applying a second algorithm to mutant, structural ECM proteins, whereby only an absolute value related to MMP7 sensitivity was calculated, no significant differences in survival between patients with relatively sensitive versus relatively insensitive mutant, ECM peptides was detected. This may be somewhat surprising given the association of high levels of MMP-7 secretion by melanoma cells with reduced survival [16].

Nevertheless, the above data did effectively identify a low-surviving set of patients with mutant ECM peptides representing an increase in MMP7 sensitivity, albeit without an overlapping assessment of absolute sensitivity. This set of low surviving patients could be explained as follows. First, the set of low surviving patients had tumors with mutant AAs in the structural ECM proteins that only represented an increase in MMP-7 sensitivity. It was not possible, or at least highly unlikely, to have a tumor with AA that led only to increased resistance, given our results that such AA substitutions are rare. However, given the high frequency of AA substitutions leading to an increase in sensitivity, and given tumors with only a few mutations, the occurrence of a relatively small number of patients with only increased sensitivity and a small number of mutations is expected. Second, as noted in the Introduction, fewer mutations means a lower anti-cancer immune response [31], and indeed, in this study, the recovery of TRB recombination reads from the exome files of the melanoma dataset examined supported this conclusion. Thus, the patients having tumors with mutant AAs leading only to an increase in MMP-7 sensitivity is thereby explained.

The association of the overall increased number of sensitive mutant AA with a higher mutation rate and better outcomes may have its technical applications. For example, because most mutant AA do increase ECM structural protein sensitivity, it would be likely only a matter of establishing MMP-7 digestion standards to make an in vitro comparison of relatively few mutations versus a high number of mutations, possibly with a microscopic assay, representing many simple alternatives. Second harmonic generation microscopy in particular is a highly convenient method for assessing ECM structural protein integrity [32]. This type of approach could be particularly important where cost-effectiveness is required, such as in repeated assessments of mutation accumulation, as in childhood chemotherapy treatment; or in settings where DNA sequencing is not practical or possible. With such an approach, it may be easier to justify use of immune checkpoint inhibitors, or other immuno-therapies, where DNA sequencing, to obtain mutation burdens is considered a guide to the use of immunotherapies, but where the DNA sequencing is not economically or technologically practical.

COI statement

Authors have nothing to declare.

Ethical statement

The above analyses is considered non-human subjects research. However, NIH approval was needed for access to TCGA WXS files, granted by NIH dbGaP project approval number 6300.

Acknowledgements

Authors wish to thank USF research computing and the taxpayers of the State of Florida.

Appendix A. Supplementary data

Supplementary data to this article can be found online at https://doi.org/10.1016/j.clinbiochem.2018.11.004.

References

[1] C. Maletzki, F. Schmidt, W.G. Dirks, M. Schmitt, M. Linnebacher, Frameshift-derived neoantigens constitute immunotherapeutic targets for patients with microsatellite-instable haematological malignancies: frameshift peptides for treating MSI + blood cancers, Eur. J. Cancer 49 (11) (2013) 2587–2595.
[2] A. Snyder, V. Makarov, T. Merghoub, J. Yuan, J.M. Zaretsky, A. Desrichard, L.A. Walsh, M.A. Postow, P. Wong, T.S. Ho, T.J. Hollmann, C. Bruggeman, K. Kannan, Y. Li, C. Elipenahli, C. Liu, C.T. Harbison, L. Wang, A. Ribas, J.D. Wolchok, T.A. Chan, Genetic basis for clinical response to CTLA-4 blockade in melanoma, N. Engl. J. Med. 371 (23) (2014) 2189–2199.
[3] B.E. Howitt, S.A. Shukla, L.M. Sholl, L.L. Ritterhouse, J.C. Watkins, S. Rodig, E. Stover, K.C. Strickland, A.D. D'Andrea, C.J. Wu, U.A. Matulonis, P.A. Konstantinopoulos, Association of polymerase e-mutated and microsatellite-instable endometrial cancers with neoantigen load, number of tumor-infiltrating lymphocytes, and expression of PD-1 and PD-L1, JAMA Oncol. 1 (9) (2015) 1319–1323.
[4] H. Westdorp, F.L. Fennemann, R.D. Weren, T.M. Bisseling, M.J. Ligtenberg, C.G. Figdor, G. Schreibelt, N. Hoogerbrugge, F. Wimmers, I.J. de Vries, Opportunities for Immunotherapy in Microsatellite Instable Colorectal Cancer, Cancer Immunology, Immunotherapy, (2016), p. CII.
[5] E. Bouffet, V. Larouche, B.B. Campbell, D. Merico, R. de Borja, M. Aronson, C. Durno, J. Krueger, V. Cabric, V. Ramaswamy, N. Zhukova, G. Mason, R. Farah, S. Afzal, M. Yalon, G. Rechavi, V. Magimairajan, M.F. Walsh, S. Constantini, R. Dvir, R. Elhasid, A. Reddy, M. Osborn, M. Sullivan, J. Hansford, A. Dodgshun, N. Klauber-Demore, L. Peterson, S. Patel, S. Lindhorst, J. Atkinson, Z. Cohen, R. Laframboise, P. Dirks, M. Taylor, D. Malkin, S. Albrecht, R.W. Dudley, N. Jabado, C.E. Hawkins, A. Shlien, U. Tabori, Immune Checkpoint Inhibition for Hypermutant Glioblastoma Multiforme Resulting from Germline Biallelic Mismatch Repair Deficiency, J. Clin. Oncol. (2016).
[6] H. Westdorp, F.L. Fennemann, R.D. Weren, T.M. Bisseling, M.J. Ligtenberg, C.G. Figdor, G. Schreibelt, N. Hoogerbrugge, F. Wimmers, I.J. de Vries, Opportunities for immunotherapy in microsatellite instable colorectal cancer, Cancer Immunol. Immunother. 65 (10) (2016) 1249–1259.
[7] Y.N. Tu, W.L. Tong, T.J. Fawcett, G. Blanck, Lung tumor exome files with T-cell receptor recombinations: a mouse model of T-cell infiltrates reflecting mutation burdens, Lab. Investig. 97 (12) (2017) 1516–1520.
[8] B.M. Callahan, J.S. Patel, T.J. Fawcett, G. Blanck, Cytoskeleton and ECM tumor mutant peptides: increased protease sensitivities and potential consequences for the HLA class I mutant epitope reservoir, Int. J. Cancer 142 (5) (2018) 988–998.
[9] S. Zaman, B.I. Chobrutskiy, J.S. Patel, B.M. Callahan, W.L. Tong, G. Blanck, Mutant cytoskeletal and ECM peptides sensitive to the ST14 protease are associated with a worse outcome for glioblastoma multiforme, Biochem. Biophys. Res. Commun. (2018).
[10] B. Xiao, D. Chen, S. Luo, W. Hao, F. Jing, T. Liu, S. Wang, Y. Geng, L. Li, W. Xu, Y. Zhang, X. Liao, D. Zuo, Y. Wu, M. Li, Q. Ma, Extracellular translationally controlled tumor protein promotes colorectal cancer invasion and metastasis through Cdc42/JNK/MMP9 signaling, Oncotarget 7 (31) (2016) 50057–50073.
[11] K. Cronin, H. Escobar, K. Szekeres, E. Reyes-Vargas, A.L. Rockwood, M.C. Lloyd, J.C. Delgado, G. Blanck, Regulation of HLA-DR peptide occupancy by histone deacetylase inhibitors, Human Vacc. Immunother. 9 (4) (2013) 784–789.
[12] N.D. Rawlings, A.J. Barrett, MEROPS: the peptidase database, Nucleic Acids Res. 27 (1) (1999) 325–331.
[13] N.D. Rawlings, Peptidase specificity from the substrate cleavage collection in the MEROPS database and a tool to measure cleavage site conservation, Biochimie 122 (2016) 5–30.
[14] N. Felli, F. Felicetti, A.M. Lustri, M.C. Errico, L. Bottero, A. Cannistraci, A. De Feo, M. Petrini, F. Pedini, M. Biffoni, E. Alvino, M. Negrini, M. Ferracin, G. Mattia, A. Care, miR-126&126* restored expressions play a tumor suppressor role by directly regulating ADAM9 and MMP7 in melanoma, PLoS One 8 (2) (2013) e56824.
[15] W. Zuidervaart, S. Pavey, F.A. van Nieuwpoort, L. Packer, C. Out, W. Maat, M.J. Jager, N.A. Gruis, N.K. Hayward, Expression of Wnt5a and its downstream effector beta-catenin in uveal melanoma, Melanoma Res. 17 (6) (2007) 380–386.
[16] K. Kawasaki, T. Kawakami, H. Watabe, F. Itoh, M. Mizoguchi, Y. Soma, Expression

of matrilysin (matrix metalloproteinase-7) in primary cutaneous and metastatic melanoma, Br. J. Dermatol. 156 (4) (2007) 613–619.
[17] A. Naba, K.R. Clauser, S. Hoersch, H. Liu, S.A. Carr, R.O. Hynes, The matrisome: in silico definition and in vivo characterization by proteomics of normal and tumor extracellular matrices, Mol. Cell. Proteomics 11 (4) (2012) M111 014647.
[18] M.L. Parry, M. Ramsamooj, G. Blanck, Big genes are big mutagen targets: a connection to cancerous, spherical cells? Cancer Lett. 356 (2) (2015) 479–482 Pt B.
[19] C. Rome, J. Arsaut, C. Taris, F. Couillaud, H. Loiseau, MMP-7 (matrilysin) expression in human brain tumors, Mol. Carcinog. 46 (6) (2007) 446–452.
[20] A. Naba, K.R. Clauser, C.A. Whittaker, S.A. Carr, K.K. Tanabe, R.O. Hynes, Extracellular matrix signatures of human primary metastatic colon cancers and their metastases to liver, BMC Cancer 14 (2014) 518.
[21] A. Naba, K.R. Clauser, J.M. Lamar, S.A. Carr, R.O. Hynes, Extracellular matrix signatures of human mammary carcinoma identify novel metastasis promoters, elife 3 (2014) e01308.
[22] Z. Ping, G.P. Siegal, J.S. Almeida, S.J. Schnitt, D. Shen, Mining genome sequencing data to identify the genomic features linked to breast cancer histopathology, J. Pathol. Informa. 5 (2014) 3.
[23] J. Gao, B.A. Aksoy, U. Dogrusoz, G. Dresdner, B. Gross, S.O. Sumer, Y. Sun, A. Jacobsen, R. Sinha, E. Larsson, E. Cerami, C. Sander, N. Schultz, Integrative analysis of complex cancer genomics and clinical profiles using the cBioPortal, Sci. Signal. 6 (269) (2013) pl1.
[24] E. Cerami, J. Gao, U. Dogrusoz, B.E. Gross, S.O. Sumer, B.A. Aksoy, A. Jacobsen, C.J. Byrne, M.L. Heuer, E. Larsson, Y. Antipin, B. Reva, A.P. Goldberg, C. Sander, N. Schultz, The cBio cancer genomics portal: an open platform for exploring multidimensional cancer genomics data, Cancer Discov. 2 (5) (2012) 401–404.
[25] A.T. Mai, W.L. Tong, Y.N. Tu, G. Blanck, T-cell receptor-alpha recombinations in renal cell carcinoma exome files correlate with an intermediate level of T-cell exhaustion biomarkers, Int. Immunol. (2018).
[26] Y.N. Tu, W.L. Tong, J.M. Yavorski, G. Blanck, Immunogenomics: a negative Prostate Cancer Outcome Associated with TcR-gamma/delta Recombinations, Cancer Microenviron. (2018).
[27] J.C. Kinskey, Y.N. Tu, W.L. Tong, J.M. Yavorski, G. Blanck, Recovery of Immunoglobulin VJ Recombinations from Pancreatic Cancer Exome Files strongly Correlates with Reduced Survival, Cancer Microenviron. (2018).
[28] Y.N. Tu, W.L. Tong, M.D. Samy, J.M. Yavorski, M. Kim, G. Blanck, Assessing microenvironment immunogenicity using tumor specimen exomes: Co-detection of TcR-alpha/beta V(D)J recombinations correlates with PD-1 expression, Int. J. Cancer (2017).
[29] E. Szymanska, M. Slowinska, S. Majewski, The role of extracellular matrix components in the T-cell activation in systemic sclerosis, Pol. Merkur. Lekarski 15 (85) (2003) 89–94.
[30] I.J. Cohen, R. Blasberg, Impact of the tumor microenvironment on tumor-infiltrating lymphocytes: focus on breast cancer, Breast Cancer (Auckl.) 11 (2017) 1178223417731565.
[31] D.B. Johnson, G.M. Frampton, M.J. Rioth, E. Yusko, Y. Xu, X. Guo, R.C. Ennis, D. Fabrizio, Z.R. Chalmers, J. Greenbowe, S.M. Ali, S. Balasubramanian, J.X. Sun, Y. He, D.T. Frederick, I. Puzanov, J.M. Balko, J.M. Cates, J.S. Ross, C. Sanders, H. Robins, Y. Shyr, V.A. Miller, P.J. Stephens, R.J. Sullivan, J.A. Sosman, C.M. Lovly, Targeted Next Generation Sequencing Identifies Markers of Response to PD-1 Blockade, Cancer Immunol. Res. 4 (11) (2016) 959–967.
[32] N.M. Clark, C.A. Garcia Galindo, V.K. Patel, M.L. Parry, R.J. Stoll, J.M. Yavorski, E.P. Pinkason, E.M. Johnson, C.M. Walker, J. Johnson, W.J. Sexton, D. Coppola, G. Blanck, The human, F-actin-based cytoskeleton as a mutagen sensor, Cancer Cell Int. 17 (2017) 121.